Broad tunability from a compact, low-threshold Cr:LiSAF laser incorporating an improved birefringent filter and multiple-cavity Gires–Tournois interferometer mirrors

Barry Stormont, Alan J. Kemp, Iain G. Cormack, Ben Agate, C. Tom A. Brown,* and Wilson Sibbett

J. F. Allen Physics Research Laboratories, School of Physics and Astronomy, University of St. Andrews, St. Andrews, KY16 9SS, Scotland

Robert Szipöcs

R&D Lézer-Optika Bt., H-1539 Budapest, P.O. Box 622, Hungary

Received December 12, 2003; revised manuscript received October 7, 2004; accepted January 4, 2005

We demonstrate prismless tuning of a compact femtosecond Cr:LiSAF laser. The employed technique, which uses a specially designed birefringent filter in combination with dispersion compensation from a pair of multiple-cavity Gires–Tournois interferometer mirrors, provides tuning over 20 nm. We give the results of theoretical modeling of the tuning velocity and the spectral width of the central passband. We show, both experimentally and theoretically, that a single birefringent plate can be used to control the oscillating bandwidth of the laser. The effect this has on the output-pulse duration has also been investigated. © 2005 Optical Society of America

OCIS codes: 320.7090, 140.4050.

1. INTRODUCTION

Cr:LiSAF is a versatile laser crystal having a high product of a stimulated-emission cross section and an upper-state lifetime that enables the construction of low-threshold and efficient laser systems.[1–3] Cr:LiSAF has a broadband emission bandwidth capable of supporting femtosecond pulses and an absorption band that is convenient for diode pumping. Thus compact femtosecond Cr:LiSAF lasers have been operated at gigahertz repetition rates[4] and have produced kilowatt peak-power levels as well as femtosecond pulses in the blue spectral region with single-pass extracavity frequency doubling.[5] Some of the laser configurations described in Refs. 1–5 suffer the common disadvantage of a fixed-center wavelength. For many applications, notably in pump-probe spectroscopy, the tuning of the center wavelength of the femtosecond pulses must be achieved over tens of nanometers. The most common approach to the tuning of a femtosecond laser involves the use of two prisms and a slit.[6,7] This technique has the inherent disadvantage that the typical prism separation increases the cavity footprint considerably. This separation also increases the amplitude noise and the jitter associated with the laser through air fluctuations shifting the beam relative to the slit. We describe here a technique for the tuning of the center wavelength of a femtosecond laser system that not only is conducive to low-threshold operation but also retains a degree of compactness that is not available with prism-based tuning techniques.

Recent years have seen considerable research into mirror-based dispersion-compensation schemes designed to provide broadband, engineerable control of dispersion in compact resonator configurations. Two design strategies that have been used with notable success are chirped mirrors[8] and multiple-cavity Gires–Tournois interferometer (GTI) (MCGTI) mirrors.[9] MCGTI mirrors consist of several GTI layers[9,10] at the front of the multilayer mirror structure. Unlike many chirped mirror designs,[11] no degradation exists in the reflectivity. This means that MCGTI mirrors are more applicable in low-threshold lasers, because they offer both attractively low-insertion losses and high per-bounce dispersion.

In this paper, a combination of MCGTI mirrors for dispersion compensation and a specially designed birefringent filter (BRF) is used to tune a femtosecond laser. Conventional birefringent filters[12] are excellent tuning elements for single-frequency lasers, but the task is rather different when one wishes to alter the center wavelength of the larger spectral width of a femtosecond laser. Naganuma *et al.*[13] have demonstrated that a birefringent plate whose optic axis is at a large angle to the surface of the plate is a suitable tuning element for a mode-locked color-center laser. We have adapted this design concept and have been able to demonstrate a filter with tuning properties more suited to a low-gain–low-threshold femtosecond Cr:LiSAF laser. We include the results of a Jones matrix analysis of the filter properties that yields such characteristics as tuning velocities and spectral passbands. An inherent property of the filter design proposed by Naganuma *et al.*,[13] and our subsequent adaptation, is that a number of passbands of varying width can be accessed by a simple azimuthal rotation of the filter. This

increased functionality can be readily exploited for control of the oscillating bandwidth of the laser. Thus a low-threshold laser with a "designer" pulse duration can be configured through the incorporation of a single intracavity birefringent plate.

The use of mirrors based on an MCGTI design enabled Golubovic *et al.*[10] to demonstrate an 80-MHz Kerr-lens mode-locked Ti:sapphire laser that has a tunability extending over 100 nm. A conventional birefringent filter consisting of a 2-mm-thick birefringent plate was used to tune the center wavelength of this laser. In the context of a low-threshold system, this plate would have seriously compromised the laser performance in the region around the center of the passband. Specifically, if this plate had been used in a Cr:LiSAF laser, it would not have retained sufficient lasing bandwidth to produce femtosecond pulses; see Fig. 1 for illustration. In this paper we show how both the filter and the mirrors can be designed to be compatible with the operational requirements of a low-threshold Cr:LiSAF laser mode locked by use of a semiconductor saturable absorber mirror (SESAM).

2. BIREFRINGENT FILTER DESIGN

A BRF comprises a thin birefringent crystal combined with a suitable polarization-dependent loss.[14] Modification of the birefringence experienced by the intracavity field changes the wavelength dependence of the intracavity loss and tuning results.

Careful design of a birefringent filter for a low-gain mode-locked laser is critical, because the shape of the resultant passband must permit oscillation on sufficient bandwidth to permit the generation of femtosecond pulses. In a low-gain system, any excess loss away from the peak-transmission wavelengths of the intracavity filter will quickly suppress laser oscillation on these wavelengths. Indeed, filters that impose large losses within their stop bands are unnecessary and undesirable in lower-gain laser oscillators, because they tend to restrict the oscillating bandwidth. It is therefore not appropriate to reference the passband to the half-maximum transmission, given that lasing will be suppressed at significantly higher levels of transmission under the conditions of low gain. Typical output coupling for low-threshold lasers is around 1% or even less, and so 99% transmission widths are a more realistic and useful reference for such systems. Figure 1 illustrates how a conventional filter of a given thickness constricts the optical bandwidth, whereas this constraint is relaxed considerably for a filter of equal thickness having a diving optic axis.

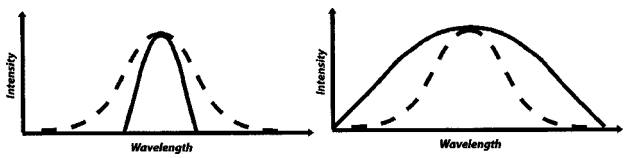

Fig. 1. Comparison between the pass band offered by the filter compared with the allowed oscillating bandwidth when a conventional filter (left) and a filter with a steeply diving optic axis (right) are used. Free-running spectral bandwidth is shown as a dashed curve, and pass bandwidth of the filter is shown as a solid curve. The filter on the right has little effect on the output spectral width of the laser. The filters described by this diagram are of similar thicknesses. A standard filter can offer the same enlarged bandwidth as a filter with a steeply diving optic axis if it is made sufficiently thin.

In a conventional BRF there is no real distinction between phase differences induced between the two polarization components where such differences are multiples of 2π (2π, 4π, $2m\pi$, etc.), but in a filter that has a steeply diving optic axis, the filter properties depend on the filter order m.[13] This manifests itself as a different spectral pass bandwidth and a different tuning velocity for each value of m. Our filter design can therefore be used to force the laser to oscillate with a particular bandwidth that directly determines the duration of the output pulses.

Naganuma *et al.*[13] extended the usual Jones matrix algebra used for describing a birefringent plate to that for a plate with a steeply diving optic axis. This work illustrated the further advantage that a filter having a steep optic-axis dive angle is considerably thicker for a given bandwidth and thus has reduced etalon effects and is more easily handled. Additionally, with a careful choice of the dive angle, broad tuning of the center wavelength can be achieved without significant deterioration in the depth of the stop band.

In contrast to the results presented by Naganuma *et al.* for color-center lasers, the need to obtain and maintain deep stop bands is an unnecessary condition for the low-gain laser described here. This enabled us to produce a filter design that incorporates the main advantages of filters with steep optic-axis dive angles but where the passband characteristics are tailored to suit a low-threshold, femtosecond Cr:LiSAF laser.

3. MODELING OF A BRF WITH A STEEPLY DIVING OPTIC AXIS

The study of optical systems that act on the polarization state of incident light, such as BRFs, can be eased by decomposing the incident field into its polarization components that can be represented in vector form.[15,16] A Jones matrix M can then be used to describe the action of each element in an optical system on the polarization state of the light. This can seen in the following equation:

$$\begin{bmatrix} E_{p,\mathrm{out}} \\ E_{s,\mathrm{out}} \end{bmatrix} = M \begin{bmatrix} E_{p,\mathrm{in}} \\ E_{p,\mathrm{in}} \end{bmatrix}, \tag{1}$$

where $E_{p,\mathrm{out}}$,$E_{s,\mathrm{out}}$ are the output electric-field components polarized in the p and s directions, respectively. M, the Jones matrix for the system, is a 2×2 matrix that describes the effect of the optical element or elements on the polarization. $E_{p,\mathrm{in}}$ and $E_{s,\mathrm{in}}$ are the input electric-field components polarized in the direction parallel to the Brewster surface, p, and the perpendicular s direction.

Figure 2 shows the important angles used to construct the Jones matrix for a filter with a steeply diving optic axis. The filter has a thickness L, and the light is incident on the filter at an angle ϕ. The optic axis of the filter makes an angle θ with respect to the surface of the plate. The azimuthal angle (the degree of freedom when used intracavity), is indicated by α.

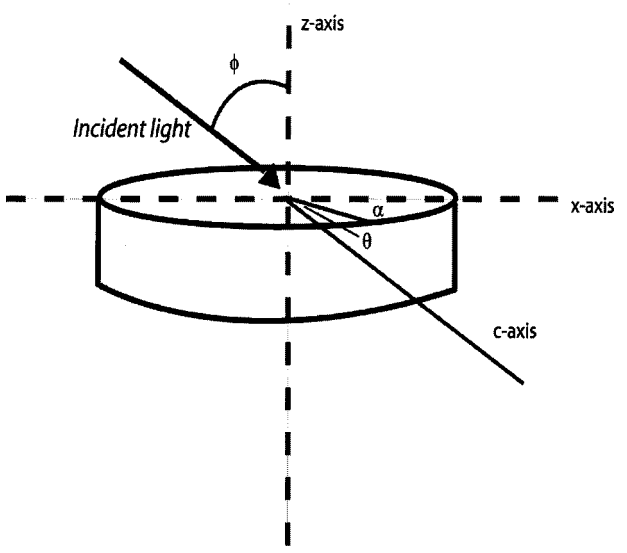

Fig. 2. Schematic showing the important angles in the filter model.

To construct the Jones matrix M, Naganuma *et al.*[13] first considered the phase difference incurred between the extraordinary and ordinary components as the light propagates through the birefringent plate. This calculation is complicated by the fact that the optic axis is not in the plane of the plate, as it would be with a conventional filter. Their results indicate a phase change between the extraordinary and ordinary components, given by

$$\Theta = f_b(k\,\delta L/\cos\,\phi), \tag{2}$$

where f_b is given by

$$f_b \equiv \sin^2\,\gamma = \cos^2\,\theta \sin^2\,\alpha + (\cos\,\phi \cos\,\theta \cos\,\alpha - \sin\,\phi \sin\,\theta)^2, \tag{3}$$

where γ is the angle between the direction of propagation and the optic axis of the crystal. For each filter order, Eq. (2) can be solved numerically to retrieve the wavelength that corresponds to a filter maximum at any particular azimuthal angle. However, to determine the spectral width of each filter maximum, the eigenvalues of the full Jones matrix for a round trip of the filter must be found. This matrix is given by

$$M = \begin{bmatrix} 1 & 0 \\ 0 & q \end{bmatrix} \begin{bmatrix} \sin\,\alpha_{eq} & \cos\,\alpha_{eq} \\ -\cos\,\alpha_{eq} & \sin\,\alpha_{eq} \end{bmatrix} \begin{bmatrix} 1 & 0 \\ 0 & e^{i\Theta} \end{bmatrix} \times \begin{bmatrix} \sin\,\alpha_{eq} & -\cos\,\alpha_{eq} \\ \cos\,\alpha_{eq} & \sin\,\alpha_{eq} \end{bmatrix} \begin{bmatrix} 1 & 0 \\ 0 & q \end{bmatrix}. \tag{4}$$

The first component matrix in this expanded Jones matrix describes the transmission of the light on entering the Brewster-angled filter. The factor q is the Fresnel coefficient for the high-loss polarization:

$$q = \frac{2n}{(n^2+1)}. \tag{5}$$

The second and fourth terms are the rotation matrices. These realign the axes of the calculation to account for the azimuthal rotation of the filter. α_{eq} is given by

$$\cos\,\alpha_{eq} = (\cos\,\phi \cos\,\theta \cos\,\alpha - \sin\,\phi \sin\,\theta)/\sin\,\gamma. \tag{6}$$

This describes the equivalent azimuthal angle and takes into account the ray propagation through the crystal. It should be noted that this simple model does not take into account the birefringence of the gain medium, although this could be done with some adaptation,[17] or the gain offered by the laser crystal. The results for several different plates can be seen in Fig. 3.

The plate having the characteristics, illustrated in Fig. 3(a), is the design used in the high-gain color-center laser as described by Naganuma *et al.*[13] This was a 1.65-mm-thick quartz plate with 66-deg optic-axis dive angle. The plate shown in Fig. 3(b) is the plate designed for and incorporated into our low-gain Cr:LiSAF laser. It was a 0.66-mm-thick quartz plate with a 57-deg optic-axis dive angle. By contrast, the plate shown in Fig. 3(c) is a regular 1-mm BRF that has its optic axis parallel to the plate surface. As Fig. 4 demonstrates and Naganuma *et al.*[13] discuss, optimization of the optic-axis dive angle to a value around 66-deg leads to the maintenance of the stop band during tuning. Whereas this is relevant to the operation of high-gain laser systems where undesired wavelengths require strong suppression, it is of considerably less importance in low-gain systems where losses of a few percent are likely to be sufficient to provide the necessary suppression. Thus it was expected that both the 66-deg and 57-deg dive angle plates would provide adequate stop-band suppression for a low-gain laser. The 57-deg optic-axis dive angle plates have the added advantage that no spatial walk-off will occur between the polarization components, because propagation is along a crystal axis. In choosing between the two filter designs, it is more important to consider the pass bandwidth and the tuning velocity. Comparison of the other two plates with that shown in Fig. 3(c) shows the difference in spectral widths for a diving axis BRF compared with that of a BRF that has its optic axis in the plane of the plate. This plate proved unusable in a low-gain femtosecond Cr: LiSAF laser because insufficient bandwidth oscillates; in fact, this plate would have to be 100 μm thick to offer the same pass bandwidth as the counterpart having the diving optic axis. The tuning velocities associated with each filter order for a 0.66-mm-thick plate having a 57-deg optic-axis dive angle plate are shown in Fig. 4. This figure shows the wavelength that will experience maximum transmission as a function of the filter azimuthal angle α. In terms of tuning velocity, the 57-deg dive angle filters are superior to the 66-deg dive angle filters in the context of low-gain femtosecond lasers. This is because each filter order tends to tune at a lower rate with the 57-deg filter compared with the 66-deg filter. For example, the first order of the Naganuma filter tunes at 45 nm/deg, whereas the 57-deg filter tunes at 40 nm/deg; the second order of the Naganuma filter tunes at 36 nm/deg, whereas the second order of the 57-deg filter tunes at 25 nm/deg. This makes the lower filter orders of the 57-deg filter a lot more usable than those of the Naganuma filter, since a lower degree of precision will be required when the 57-deg filter is filtered.

The data plotted in Fig. 4 show that as the filter order increases, the tuning velocity decreases. This is useful in

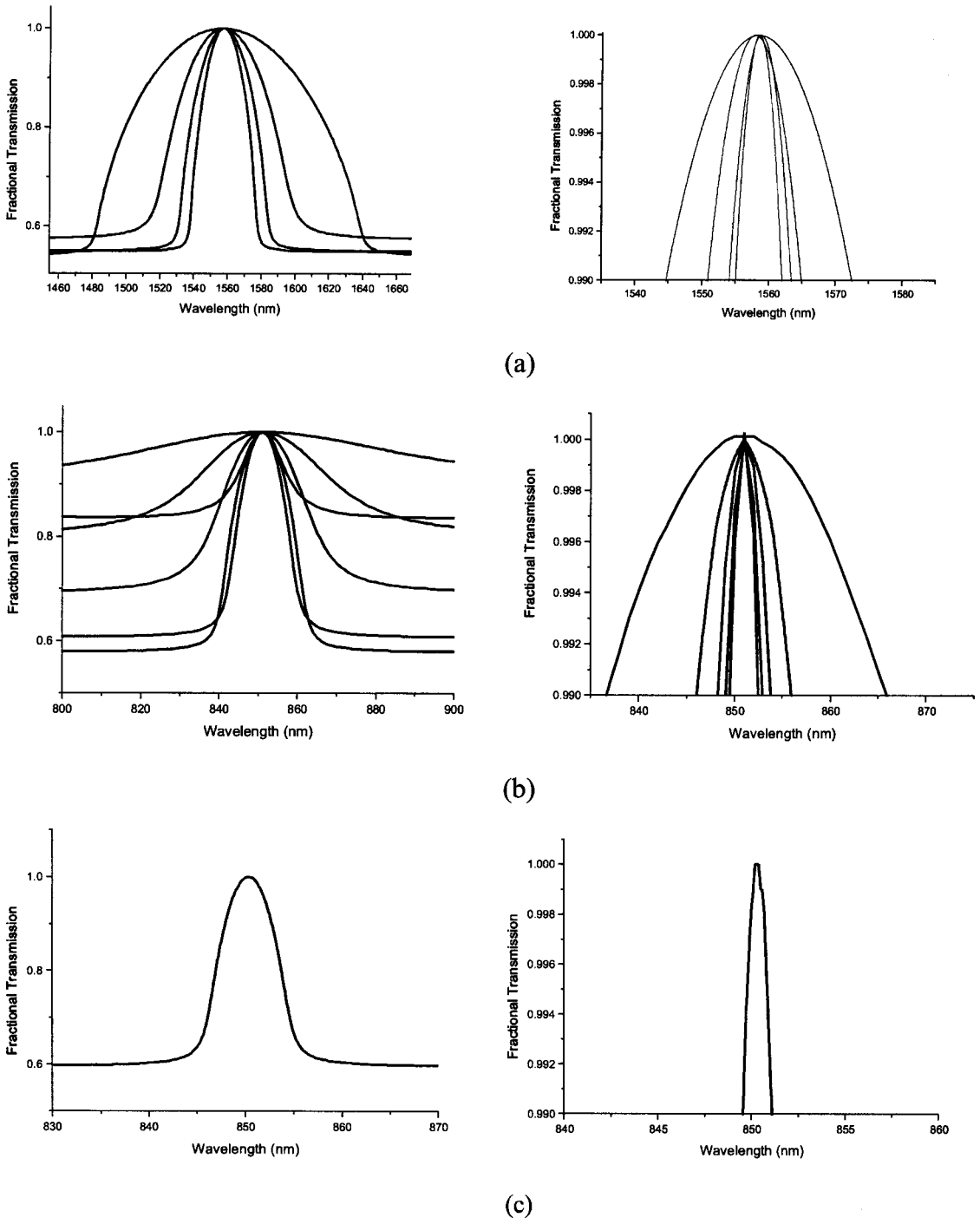

Fig. 3. (a) Spectral widths of the first four filter orders of a 1.85-mm-thick quartz birefringent plate with a 66-deg optic axis dive angle, the filter described in Naganuma *et al.* The full spectral width is shown on the left, and the 99% width is shown on the right. The first filter order has the broadest spectral bandwidth, and the fourth filter order has the narrowest. (b) Spectral widths associated with the first six filter orders of a 0.66-mm-thick quartz birefringent plate with a 57-deg optic axis dive angle and the plate used in a low-threshold Cr:LiSAF laser. The full spectral width is shown on the left, and the 99% width right on the right. The first filter order has the broadest spectral bandwidth and the sixth filter has the narrowest. (c) Spectral width of a conventional 1000-μm-thick quartz plate with a 0-deg optic axis dive angle (i.e., no dive). The full spectral width is shown on the left, and the 99% width is shown on the right.

an experimental situation in which the tuning velocity gives a reliable indication of which filter order is being used. With these parameters calculated, the 57-deg plate was used to tune a low-threshold Cr:LiSAF laser, and in Section 4 the experimental observations are described and compared with the theoretical predictions.

4. TUNING A LOW-THRESHOLD Cr:LiSAF LASER WITH A 57°, 0.66-mm QUARTZ PLATE

A laser was constructed (see Fig. 5) in much the same way as described in Ref. 3. This laser offered the widest tuning

range of all of the cavities and MCGTI mirror combinations that we evaluated. A total of three bounces per round trip on the MCGTI mirrors (two bounces on one mirror and one on the other) was found empirically to optimize system performance. The laser had a total incident pump power of 180 mW and an overall electrical-to-optical efficiency of around 1%. When mode locked with a SESAM element included in the laser cavity, this laser produced bandwidth-limited pulses of around 150-fs duration at an average output power of around 40 mW. The free-running (i.e., with no BRF in place) center wavelength was 840 nm with a bandwidth of 5 nm.

The plots in Fig. 6 show the change in the center wavelength and the output power of the cw laser (i.e., with a high-reflecting mirror in place of the SESAM) as the filter was rotated. The theoretical predictions of the tuning velocity for the first and second orders are 40 mm/deg and 25 mm/deg, respectively, but the experimentally obtained tuning velocities were 10 nm/deg and 19 nm/deg. The most likely explanation for this discrepancy is that these two filter orders have the widest pass bands (29 and 10 nm full width at 99% transmission, respectively). Consequently, the center wavelength is not tightly constrained by the filter, at least around the center of the passband, and may be considerably influenced by the gain–loss balance characteristic of the free-running laser, particularly toward the edges of its tuning range. This is evident in the s-shape of the tuning curves associated with the lower orders of the filter. This shape demonstrates that for these lower orders, the filter constrains only the oscillating wavelengths rather weakly. For any given system configuration, the laser will operate on those wavelengths exhibiting the largest net gain. Thus, when the center wavelength of the filter is tuned toward the wings of the gain bandwidth of the gain medium and a broad filter bandwidth constrains the wavelength only weakly, the highest net gain may no longer occur at the center wavelength of the filter (where the loss is minimized) but at wavelengths closer to the gain peak for the gain medium. This causes the s-shape in the tuning

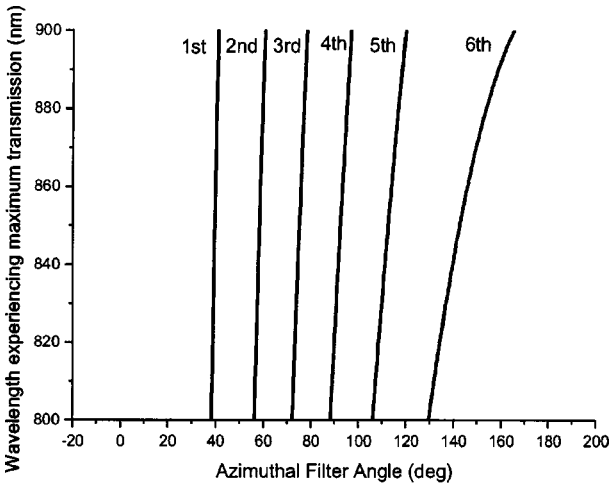

Fig. 4. Theoretical tuning velocities for the first six filter orders of a 0.66-mm-thick quartz plate with a 57-deg optic axis. First order, 40 nm/deg; second order, 25 nm/deg; third order, 17 nm/deg; fourth order, 12 nm/deg; fifth order, 7 nm/deg; sixth order, 3 nm/deg.

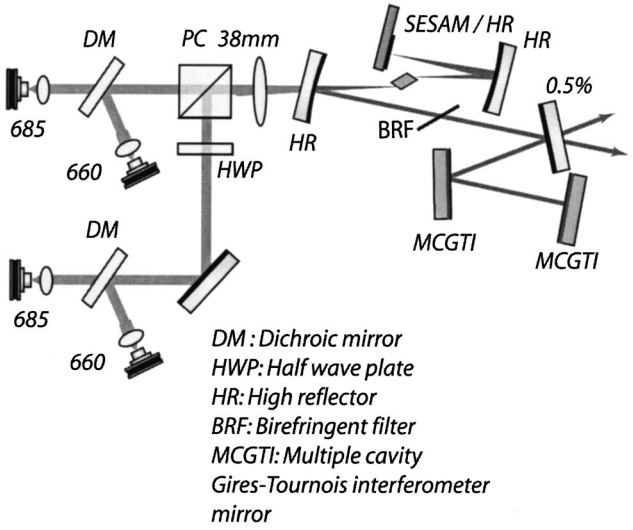

Fig. 5. Laser cavity used for the tuning experiments.

curve. It should be noted that the model described earlier does not account for this gain–loss effect from each intracavity element, because the effects of wavelength dependent gain in the laser are not included—it is a cold-cavity model. By contrast, filter orders 3–6 show very good agreement between the theoretical tuning velocity and that obtained experimentally (see Table 1). These orders have the slowest tuning velocities and the narrowest pass bands. This inevitably means that there will be a higher degree of constraint on the center wavelength. These measurements of tuning velocity in the cw laser regime identify the filter order used.

It can be seen from Fig. 6 that in a cw laser configuration these filters can tune the Cr:LiSAF laser over a spectral region exceeding 80 nm in most cases. This is certainly influenced, as expected, by the reflectivity bandwidth of the mirror set used. However, the tuning range is predominately controlled by the variation in stimulated emission cross section, and hence gain, across this wavelength range.

A comparison between the theoretical tuning velocities and the experimentally obtained values can be found in Table 1. In this table, a direct correlation between the theoretical and experimental tuning velocities for the higher filter orders can be seen, whereas for the lower filter orders the agreement is not so good, for the reasons described earlier.

When the SESAM element replaced the high-reflectivity mirror in the focused arm of the laser shown in Fig. 5, the laser could be mode locked over a tuning range of 20 nm. Our observations indicated that this tuning latitude was limited by dispersion rather than by the spectral characteristics of the saturable absorption of the SESAM.[18] This conclusion is reinforced by a similar experiment carried out with a single prism as a tuning element where 50 nm of tuning of the center wavelength corresponded almost exactly to the reflectivity of the SESAM back mirror.[5] A simple model for the intracavity dispersion was built up with the theoretical predictions for a reflection from the SESAM,[19] the measured dispersion of the MCGTI mirrors and the laser crystal,[20] the well-

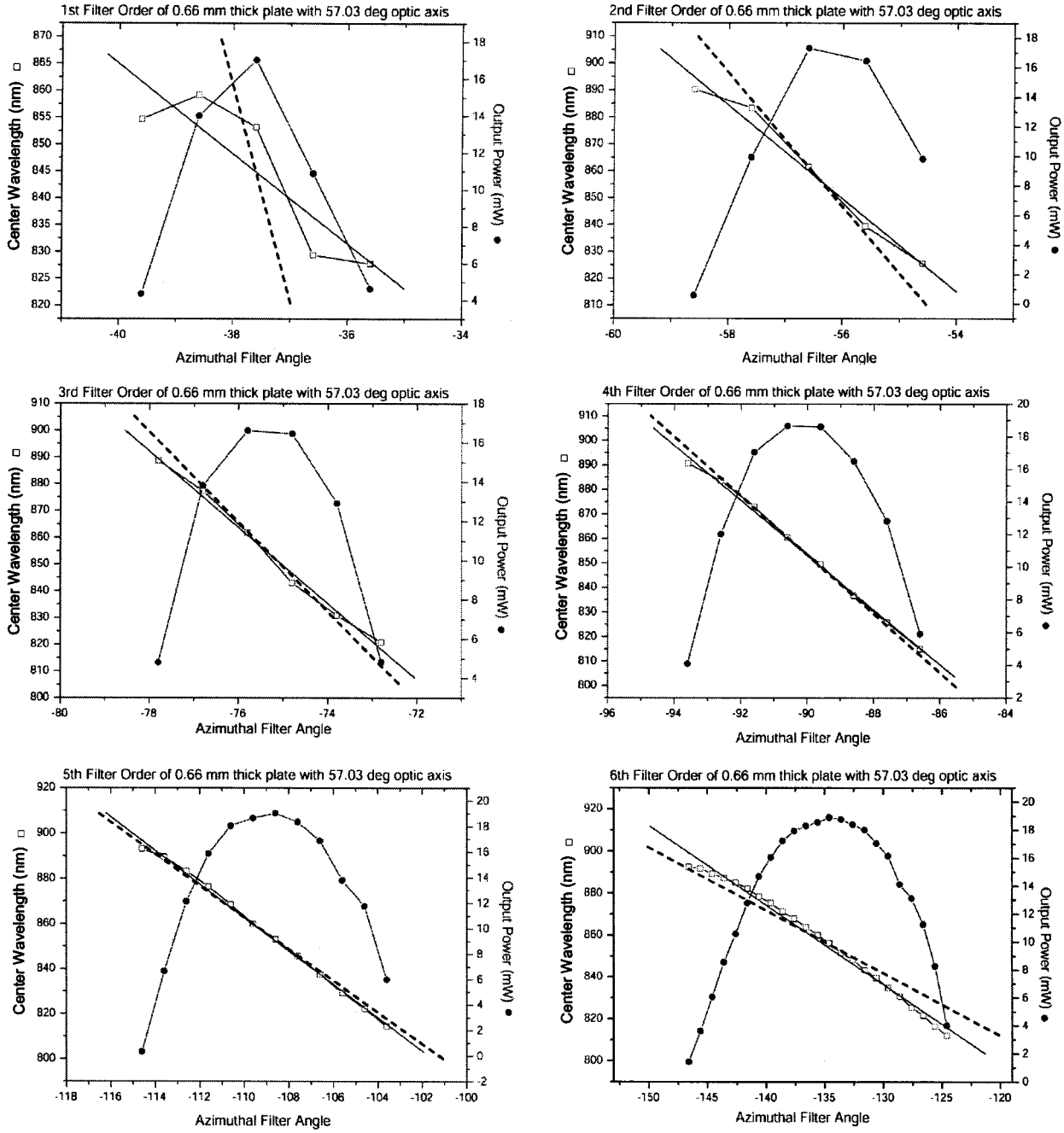

Fig. 6. cw tuning characteristics for the first six filter orders of a 0.66-mm-thick quartz plate with a 57-deg optic axis. Output power (solid circles) and center wavelength (open squares) are shown as a function of the azimuthal angle. The solid curves are fits to the experimental tuning data; the dashed lines represent the theoretical tuning velocity.

known Sellmeier equations for quartz, and the theoretical dispersion curves supplied by the manufacturer for the intracavity folding mirrors. It can be seen from the plots of tunability and dispersion in Fig. 7 that the round-trip dispersion in the cavity is substantially negative for the wavelength range within which the laser mode locks, as one might expect in a laser containing a SESAM under the conditions for soliton mode locking. Interestingly, this raises the question of whether or not the pulses would get significantly shorter if the laser could be tuned to around 865 nm, where the third-order dispersion approaches zero. However, it should be noted that optimization of

Table 1. Comparison of cw Experimental and Theoretical Tuning Velocities

Filter Order	Tuning Velocity (Experimental)	Tuning Velocity (Theoretical)
1	10 nm/deg	40 nm/deg
2	19 nm/deg	25 nm/deg
3	14 nm/deg	17 nm/deg
4	11.6 nm/deg	12 nm/deg
5	7.4 nm/deg	7 nm/deg
6	3.7 nm/deg	3 nm/deg

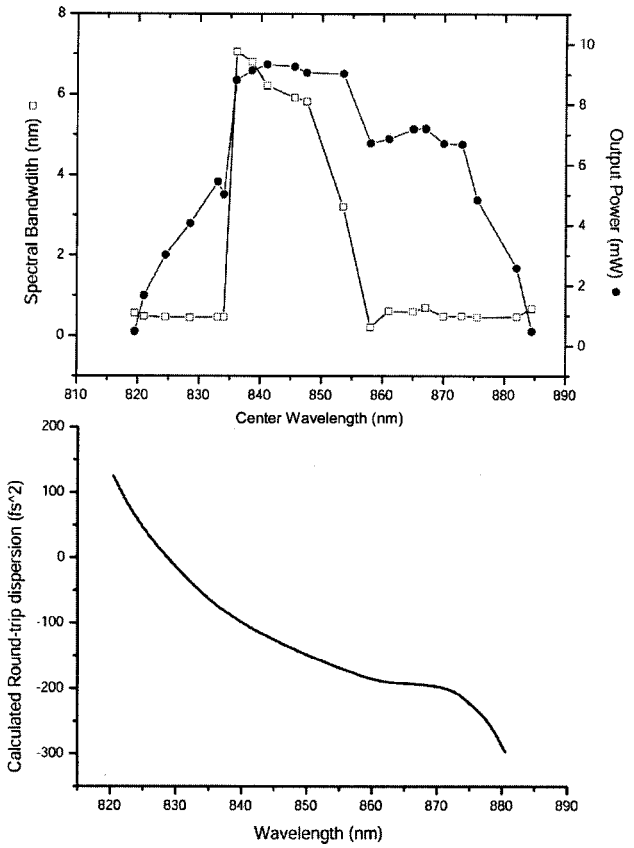

Fig. 7. Calculated round-trip dispersion (bottom) and the experimentally measured change in pulse properties (top) over 20 nm of center wavelength tuning. Output power is shown with closed circles, and spectral bandwidth is shown with open squares.

both the GDD and third-order dispersion for very short pulses would be difficult with MCGTI mirrors. This could be overcome by use of a combination of both MCGTI mirrors and GTI mirrors to ensure constant GDD over the entire laser bandwidth. However, the number of reflections required to do this would be detrimental to both the threshold pump power and the efficiency of the laser system. The dispersive properties of the BRF used away from a transmission maximum are not included in the model for the round-trip GDD. This may become important during tuning with the lower filter orders where the center wavelength of the pass band does not coincide with the center wavelength of the filter maximum. This will influence the round-trip dispersion in much the same way as does an intracavity low-finesse Fabry–Perot filter.

Also shown in Fig. 7 is the change in spectral bandwidth and output power over several tens of nanometers of tuning with the second filter order. The laser is mode locked between 840 and 860 nm, where the spectral bandwidth and the output power increase significantly.

The effect of constriction of optical bandwidth using higher filter orders was then investigated. From the filter model [see Fig. 3(b)], it can be seen that as the filter order increases, the spectral width of the pass band decreases. The SESAM was inserted, and the achieved maximum bandwidth was then monitored as the laser was tuned over its entire tuning range. Figure 8 shows the maximum spectral bandwidth that could be achieved during tuning, with each filter order plotted alongside the theoretical 99% width of the pass band associated with each filter order. As can seen from Fig. 8, the filter constricts the mode-locked operating bandwidth of the laser to a value similar to the 99% width of a given filter order. The free-running mode-locked bandwidth of the laser is significantly less than the 99% width of the first filter order, and so the laser bandwidth is readily accommodated by the first-order transmission.

The pulse durations for the 20-nm tuning range were measured for investigation of the change in pulse duration and related temporal properties as the laser is forced to change its center wavelength and hence its round-trip dispersion characteristics. Figure 9 shows the difference in pulse duration over ~20 nm of center wavelength tuning during tuning using the second filter order, and for comparison, the fourth filter order. As is immediately evident, the pulse duration achieved with the second filter order, the order that allowed the greater bandwidth to be transmitted, is significantly shorter than the pulse duration achieved with the fourth filter order. In the case of the second filter order, the minimum pulse duration that could be achieved was around 130 fs. This is the same pulse duration as was found with the free-running laser containing the MCGTI mirrors, whereas the minimum pulse duration that could be achieved with the fourth filter order was 260 fs. Shown on the same graph is the time–bandwidth product measured over this tuning range. This varies as the laser is tuned over 20 nm in both cases. It does, however, have the same excursion in both cases, which leads us to believe that the filter order used has very little effect on the chirp of the output pulse; this appears to be determined by the net dispersion seen by the pulse and is strongly dependent on the center wavelength and the bandwidth. This means that we have demonstrated a method of constraining a low-threshold femtosecond laser to oscillate with a particular frequency bandwidth and hence have forced the laser to produce output pulses of a duration defined by this constrained bandwidth.

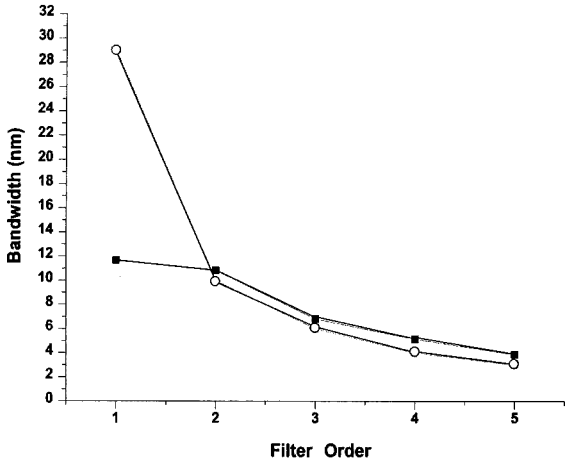

Fig. 8. Maximum bandwidth achievable with each filter order (squares) shown alongside the 99% width of the filter order (circles).

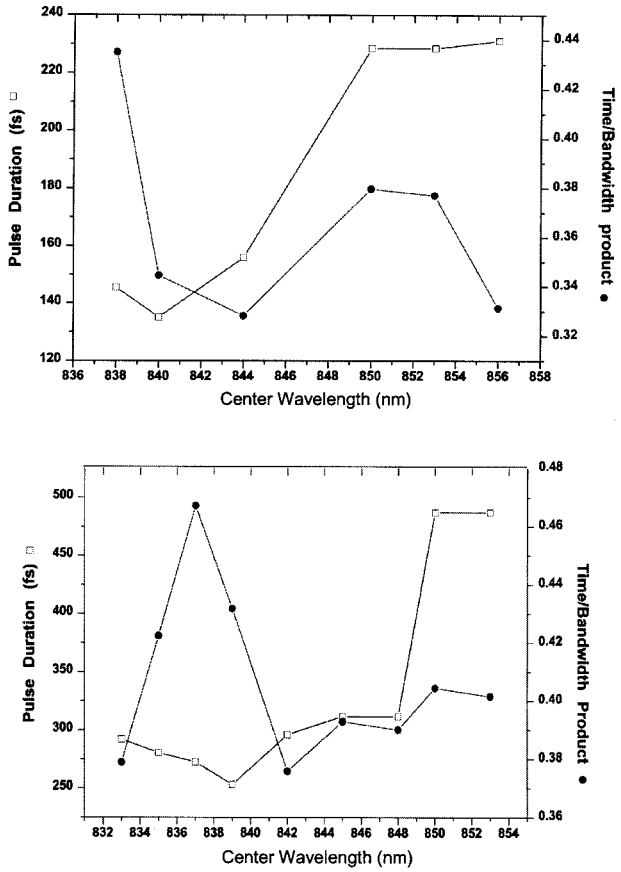

Fig. 9. Change in pulse duration when tuning is performed with the second filter order (top) and with the fourth filter order (bottom). Pulse duration is shown as open squares and time/bandwidth product is shown as closed circles.

5. CONCLUSIONS

In this paper, a technique for tuning a compact femtosecond Cr:LiSAF laser that uses the combination of MCGTI mirrors and a specifically designed birefringent filter is demonstrated. This filter is able to support femtosecond pulses with the tunability of the center wavelength of 20 nm. This tuning is limited by the round-trip dispersion provided by the MCGTI mirrors. The specially designed filter was developed with the low-gain Cr:LiSAF material in mind and so had very broad 99% transmission widths at the expense of the suppression of the neighboring wavelengths. The properties of the filter were studied, and it was found that the oscillating bandwidth of the laser could be controlled simply through the rotation of the intracavity plate. The implications this has for the pulse duration were found to be that the magnitude of the chirp on the pulse remains unaffected when a different filter order is used, and the constriction meant that near-bandwidth-limited pulses of a different pulse duration were produced.

*Telephone, +44 1334463129; fax, +44 1334 463104; e-mail, ctab@st-and.ac.uk.

REFERENCES

1. J. M. Hopkins, G. J. Valentine, W. Sibbett, J. A. der Au, F. Morier-Genoud, U. Keller, and A. Valster, "Efficient, low-noise, SESAM-based femtosecond Cr^{3+}:$LiSrAlF_6$ laser," Opt. Commun. **154**, 54–58 (1998).
2. J. M. Hopkins, G. J. Valentine, B. Agate, A. J. Kemp, U. Keller, and W. Sibbett, "Highly compact and efficient femtosecond Cr:LiSAF lasers," IEEE J. Quantum Electron. **38**, 360–368 (2002).
3. B. Agate, B. Stormont, A. J. Kemp, C. T. A. Brown, U. Keller, and W. Sibbett, "Simplified cavity designs for efficient and compact femtosecond Cr:LiSAF lasers," Opt. Commun. **205**, 207–213 (2002).
4. A. J. Kemp, B. Stormont, B. Agate, C. T. A. Brown, U. Keller, and W. Sibbett, "Gigahertz repetition-rate from directly diode-pumped femtosecond Cr:LiSAF laser," Electron. Lett. **37**, 1457–1458 (2001).
5. B. Agate, A. J. Kemp, C. T. A. Brown, and W. Sibbett, "Efficient, high repetition-rate femtosecond blue source using a compact Cr:LiSAF laser," Opt. Express **10**, 824–831 (2002).
6. D. Kopf, G. J. Spuhler, K. J. Weingarten, and U. Keller, "Mode-locked laser cavities with a single prism for dispersion compensation," Appl. Opt. **35**, 912–915 (1996).
7. R. L. Fork, O. E. Martinez, and J. P. Gordon, "Negative dispersion using pairs of prisms," Opt. Lett. **9**, 150–152 (1984).
8. N. Matuschek, F. X. Kartner, and U. Keller, "Analytical design of double-chirped mirrors with custom-tailored dispersion characteristics," IEEE J. Quantum Electron. **35**, 129–137 (1999).
9. R. Szipocs, A. Kohazi-Kis, S. Lako, P. Apai, A. P. Kovacs, G. DeBell, L. Mott, A. W. Louderback, A. V. Tikhonravov, and M. K. Trubetskov, "Negative dispersion mirrors for dispersion control in femtosecond lasers: chirped dielectric mirrors and multi-cavity Gires–Tournois interferometers," Appl. Phys. B: Lasers Opt. **70**, S51–S57 (2000).
10. B. Golubovic, R. R. Austin, M. K. Steiner-Shepard, M. K. Reed, S. A. Diddams, D. J. Jones, and A. G. Van Engen, "Double Gires–Tournois interferometer negative-dispersion mirrors for use in tunable mode-locked lasers," Opt. Lett. **25**, 275–277 (2000).
11. R. Szipocs and A. Kohazi-Kis, "Theory and design of chirped dielectric laser mirrors," Appl. Phys. B **65**, 115–135 (1997).
12. A. Yariv, *Optical Electronics* (Saunders, Fort Worth, Tex., 1991).
13. K. Naganuma, G. Lenz, and E. P. Ippen, "Variable bandwidth birefringent filter for tunable femtosecond lasers," IEEE J. Quantum Electron. **28**, 2142–2150 (1992).
14. O. Svelto, *Principles of Lasers*, 4th ed. (Plenum, New York, 1998).
15. S. Lovold, P. F. Moulton, D. K. Killinger, and N. Menyuk, "Frequency tuning characteristics of a *Q*-switched Co:MgF_2 laser," IEEE J. Quantum Electron. **21**, 202–208 (1985).
16. G. Holtom and O. Teschke, "Design of a birefringent filter for high power dye-lasers," IEEE J. Quantum Electron. **10**, 577–579 (1974).
17. A. J. Kemp, G. J. Friel, T. K. Lake, R. S. Conroy, and B. D. Sinclair, "Polarization effects, birefringent filtering, and single-frequency operation in lasers containing a birefringent gain crystal," IEEE J. Quantum Electron. **36**, 228–235 (2000).
18. D. Kopf, A. Prasad, G. Zhang, M. Moser, and U. Keller, "Broadly tunable femtosecond Cr:LiSAF laser," Opt. Lett. **22**, 621–623 (1997).
19. M. Mazilu, A. Miller, and V. T. Donchev, "Modular method for calculation of transmission and reflection in multilayered structures," Appl. Opt. **40**, 6670–6676 (2001).
20. S. Uemura, "Dispersion compensation for a femtosecond Cr:LiSAF laser," Jpn. J. Appl. Phys., Part 1 **37**, 133–134 (1998).